# Two-directional lasing from a dye-doped two-dimensional hexagonal photonic crystal made of holographic polymer-dispersed liquid crystals

D. Luo,[1] X. W. Sun,[1,a)] H. T. Dai,[1] Y. J. Liu,[2] H. Z. Yang,[3] and W. Ji[3]
[1]*School of Electrical and Electronic Engineering, Nanyang Technological University, Nanyang Avenue, Singapore 639798, Singapore*
[2]*Department of Engineering Science and Mechanics, The Pennsylvania State University, University Park, Pennsylvania 16802, USA*
[3]*Department of Physics, National University of Singapore, 2 Science Drive 3, Singapore 117542, Singapore*

(Received 15 August 2009; accepted 29 September 2009; published online 16 October 2009)

Lasing actions are demonstrated in two high-symmetry directions ($\Gamma M$ and $\Gamma K$) of a two-dimensional hexagonal photonic crystal from dye-doped holographic polymer-dispersed liquid crystals. The group velocity anomaly, which is peculiar to two-dimensional and three-dimensional photonic crystals, leads to substantial enhancement in local fields in the two-dimensional photonic crystal with a low-index contrast. The difference on the lasing thresholds between the two directions is interpreted as the result of different group velocities of the flat bands where laser oscillation occurred. © *2009 American Institute of Physics*. [doi:10.1063/1.3251078]

Photonic crystals (PCs) are artifical optical materials for controlling and manipulating the flow of light.[1,2] Due to the electrically switchable/tunable ability, holographic polymer-dispersed liquid crystals (H-PDLCs) have received much attention.[3] Thus far, two-dimensional (2D) and three-dimensional (3D) PCs have been demonstrated.[4,5] The existence of the bandgaps in PCs can result in a low group velocity at the bandgap edge, which could lead to large local-field enhancement in a gain medium.[6] In general, H-PDLC PCs cannot show complete photonic bandgaps due to the low refractive index contrast; however, local-field enhancement is still possible through the group-velocity anomaly,[7] where the group velocity becomes small over a wide range of wave vectors. The group-velocity anomaly, absent in one-dimensional (1D) case, is peculiar to 2D and 3D PCs and even exists in PCs with rather small index contrast.

The reported H-PDLC-based laser emissions were mainly from dye-doped reflection[8] or transmission gratings,[9,10] where the underlying mechanism is much similar to conventional 1D distributed feedback lasers.[11] Laser oscillation phenomena from 2D PCs are reported using dye-doped materials including semiconductors,[12–14] polymer,[15–17] and PbO glass.[18] For H-PDLC materials, only 2D PC with square lattice has been demonstrated previously.[19] In this paper, we report the lasing actions from 2D H-PDLC PCs with a hexagonal lattice structure. Two-directional lasers are observed in two high-symmetry directions ($\Gamma M$ and $\Gamma K$); small group velocity due to group-velocity anomalies is responsible for the lasing.

In our experiment, the LC/prepolymer mixture syrup used to fabricate the dye-doped 2D PC with hexagonal lattice structure was consisted of 53.10 wt % monomer, trimethylolpropane triacrylate, 13.14 wt % cross-linking monomer, *N*-vinylpyrrollidone, 0.72 wt % photoinitiator, Rose Bengal, 1.09 wt % coinitiator, *N*-phenylglycine, 10.95 wt % sur-factant, octanoic acid, and 1.82 wt % lasing dye, 4-dicyanomethylene-2-methyl-6-*p*-dimethylaminostyryl-4*H*-pyran (DCM), all from Sigma-Aldrich, and 19.18 wt % liquid crystal, E7 ($n_o$=1.5216 and $n_e$=1.7462), from Merck. The mixture was sandwiched in a cell, which was formed by two pieces of indium tin oxide coated glass.

The 2D PC was holographically fabricated through the three-beam interference based on a single prism. Figure 1(a) shows the schematic of the prism used. The bottom plane (equilateral triangle) of the prism has a side length of BC=BD=CD=6 cm, and a side-bottom plane angle of $\Phi$=60°. A collimated Ar+ laser beam (514.5 nm) impinged normally onto the prism, and three beams, $k_1$, $k_2$, and $k_3$ [Fig. 1(b)] emerged through the refraction from three tilted side surfaces of the prism. In Fig. 1(b), $k$ represents wave vector, $\theta$ represents the angle between the wave vector and $z$ axis, and $\varphi$ represents the angle between the projection of wave vector on $x$-$y$ plane and $x$ axis. Here we have $\theta_1=\theta_2=\theta_3=\theta$=25.3° and $\varphi_1$=0°, $\varphi_2$=120°, and $\varphi_3$=240°. These three beams overlapped at the bottom surface of the prism and generated an interference pattern. The cell filled with LC/prepolymer mixture was attached onto the bottom surface using an index-matching liquid to record the interference pattern, as shown in Fig. 1(c).

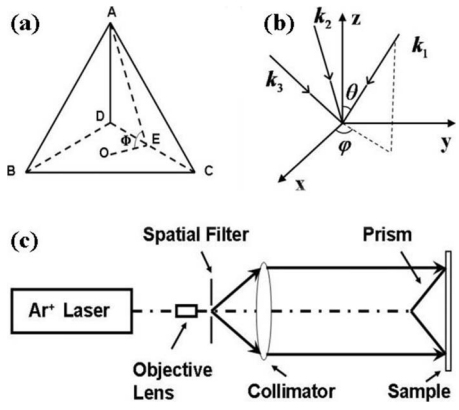


FIG. 1. (a) The specially designed prism, (b) three-beam interference configuration, and (c) schematic of the optical setup.

a)Author to whom correspondence should be addressed. Electronic mail: exwsun@ntu.edu.sg.

 

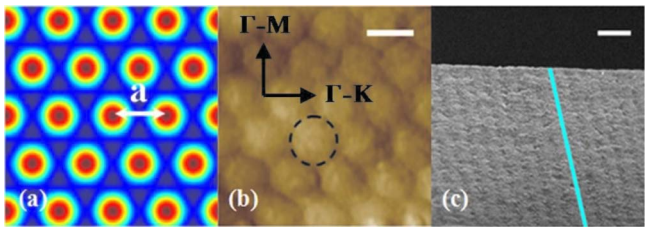


FIG. 2. (Color online) (a) Simulated intensity distribution of the three-beam interference pattern. (b) AFM image showing the surface morphology of the 2D hexagonal H-PDLC PCs. Scalar bar: 500 nm. (c) The cross-section SEM image of H-PDLC sample. Scalar bar: 1 $\mu$m.

Assuming the three beams have the same phase, the intensity distribution of the interference pattern can be defined as

$$I(r) = \Re\left\{\sum_{i,j=1}^{3} E_i \cdot E_j \exp[i(k_i - k_j)\cdot r]\right\}, \quad (1)$$

where $E$ is the amplitude, $r=(x,y,z)$ is a position vector, and $\Re[\ldots]$ denotes the real part of the argument. For three beams with equal intensity, $E_1=E_2=E_3$, the simulated interference pattern in $x$-$y$ plane is shown in Fig. 2(a), where the red-colored and blue-colored areas represent high and low intensities, corresponding to polymer-rich and LC-rich regions, respectively, when it was recorded in the PDLCs. The lattice constant [shown in Fig. 2(a)] in $x$-$y$ plane is given by $a=2\lambda/(3n\sin\theta)$. In our experiments, $\lambda=514.5$ nm, $n=1.537$ (calculated according to the ratio of polymer and LC), and $\theta=25.3°$; the theoretical lattice constant $a$ is about 522 nm.

During the polymerization process, monomers start to photopolymerize in high intensity regions, while LCs diffuse into low intensity region, thus forming the columnar polymer and LC droplets after the phase separation. The exposure intensity of each beam and exposure time were $\sim 5$ mW/cm$^2$ and 120 s, respectively. The recording area of the 2D PC sample was about $5\times 5$ mm$^2$ in $x$-$y$ plane with the thickness of 7 $\mu$m. Figure 2(b) shows the surface morphology of the 2D H-PDLC PC with a hexagonal lattice structure checked by an atomic force microscope (AFM). The lattice constant was $\sim$500 nm and the polymer columns (marked by the dashed circle) have a radius of $\sim$145 nm. Considering a general 5% volume shrinkage for acrylate monomers during photopolymerization,[20] the experimental lattice constant (500 nm) was in good agreement with the prediction (522 nm). Figure 2(c) shows a scanning electron microscopy (SEM) image of the cross-section morphology of the 2D H-PDLC PC, where the polymer columnar structure was observed along $z$ direction. The morphology of the grating is slightly slanted due to a tilted SEM observation direction.

Laser emissions along both $\Gamma M$ ($y$ axis) and $\Gamma K$ ($x$ axis) directions [Fig. 2(b)] in the sample took place when it was optically excited by a $Q$-switched frequency-doubled Nd:yttrium aluminum garnet pulsed laser operating at 532 nm with a pulse duration of 7 ns and a repetition rate of 10 Hz. A linearly polarized pumping laser, focused by a cylinder lens, was incident on the surface of sample along the $z$ direction with the transverse electric (TE) field in $x$-$y$ plane. A fiber-coupled spectrometer with a resolution of 0.6 nm was used to collect output lasing beams. The laser emission are expected to happen above 600 nm because there is an overlapping range in 500–590 nm for both absorption and photoluminescence spectra of DCM.[10]

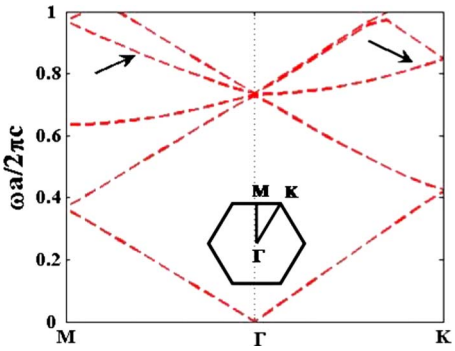


FIG. 3. (Color online) Photonic band structure of the 2D hexagonal H-PDLC PC for the TE polarization. The inset represents the irreducible Brillouin zone. Arrows show the located frequencies where the lasing action occurs.

Figure 3 shows the calculated photonic band structures for TE polarization in the 2D hexagonal HPDLC PC using the plane wave expansion method,[21] where the parameters used were $r=0.29a$, $n_p=1.522$, and $n_{LC}=1.597$. The laser emission occurred at 607 and 611 nm (Fig. 4), corresponding to the normalized frequency of $\omega a/2\pi c=0.824$ and 0.818 along $\Gamma M$ and $\Gamma K$ directions, respectively (Fig. 3). From Fig. 3, we can see that the bands, where the lasing happened along $\Gamma M$ and $\Gamma K$ directions, respectively, are relatively flat, indicating the small group velocities. In a gain medium, a small group velocity $v_g$ causes a long effective gain length,[6] where the gain is inversely proportional to $v_g$,[18] and thus leads to a large enhancement in local fields: light amplification.[7] Therefore, the laser emission was induced by the group-velocity anomalies in flat photonic bands.

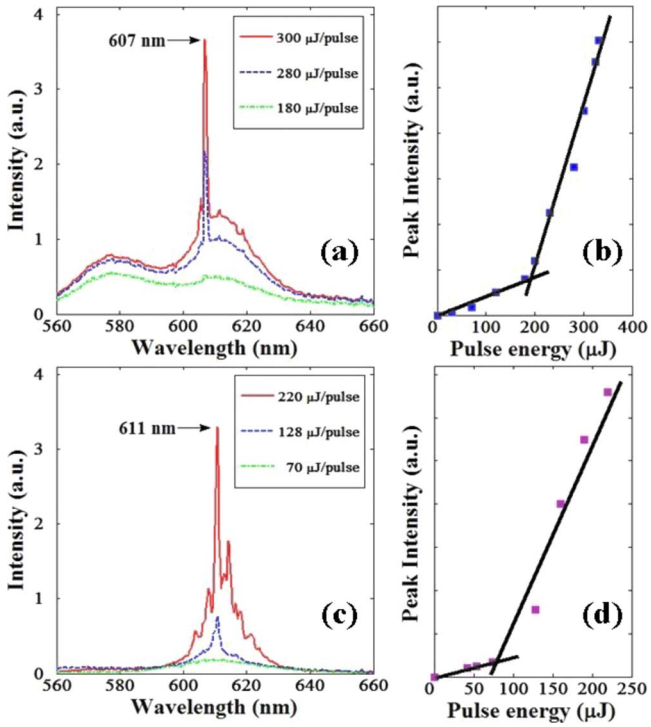


FIG. 4. (Color online) Lasing spectra measured along (a) $\Gamma M$ and (c) $\Gamma K$ directions. Relationships of peak intensity vs pumping energy along (b) $\Gamma M$ and (d) $\Gamma K$ directions.

Figure 4(a) shows the lasing spectra measured along $\Gamma M$ direction under different pumping energies. The lasing peak centers at 607 nm with a linewidth of 1.5 nm. The peak intensity as a function of pumping energy is illustrated in Fig. 4(b). The threshold of 180 $\mu$J/pulse is achieved. The same measurements along $\Gamma K$ direction were carried out, as shown in Figs. 4(c) and 4(d). There were no significant polarization characteristics in both $\Gamma M$ and $\Gamma K$ directions. Compared with $\Gamma M$ case, a slightly redshifted lasing peak occurs at 611 nm with the linewidth of 1.6 nm [Fig. 4(c)], and a much lower threshold of about 70 $\mu$J/pulse is obtained [Fig. 4(d)]. The laser threshold is proportionally related to the group velocity.[22] From Fig. 3, the band along $\Gamma K$ direction is much flatter than that along $\Gamma M$ direction, which induces a smaller group velocity but a larger enhancement in the local fields, thereby leading to a lower threshold. It is also worth mentioning that besides the primary peak, several other competing peaks appeared in the spectra along both $\Gamma M$ and $\Gamma K$ directions due to the spatial hole burning effect[17] when the pumping energy was increased far beyond the threshold [red curves in Figs. 4(a) and 4(c)].

In conclusion, we demonstrated lasing actions along both $\Gamma M$ and $\Gamma K$ directions from a DCM dye-doped 2D hexagonal H-PDLC PC. The group velocity anomaly was the underlying mechanism for the substantial light amplification in our 2D H-PDLC PCs with the low-index contrast. The big difference on the laser threshold along $\Gamma M$ and $\Gamma K$ directions was explained through the proportional relationship of the laser oscillation threshold and the group velocity of the corresponding band.

[1]E. Yablonovitch, Phys. Rev. Lett. **58**, 2059 (1987).
[2]J. D. Joannopoulos, R. D. Meade, and J. N. Winn, *Photonic Crystals: Molding the Flow of Light* (Princeton University Press, Princeton, 1995).
[3]T. J. Bunning, L. V. Natarajan, V. P. Tondiglia, and R. L. Sutherland, Annu. Rev. Mater. Sci. **30**, 83 (2000).
[4]Y. J. Liu and X. W. Sun, Appl. Phys. Lett. **89**, 171101 (2006).
[5]R. L. Sutherland, V. P. Tondiglia, L. V. Natarajan, S. Chandra, D. Tomlin, and T. J. Bunning, Opt. Express **10**, 1074 (2002).
[6]J. P. Dowling, M. Scalora, M. J. Bloemer, and C. M. Bowden, J. Appl. Phys. **75**, 1896 (1994).
[7]K. Sakoda, Opt. Express **4**, 167 (1999).
[8]G. S. He, T.-C. Lin, V. K. S. Hsiao, A. N. Cartwright, P. N. Prasad, L. V. Natarajan, V. P. Tondiglia, R. Jakubiak, R. A. Vaia, and T. J. Bunning, Appl. Phys. Lett. **83**, 2733 (2003).
[9]R. Jakubiak, L. V. Natarajan, V. Tondiglia, G. S. He, P. N. Prasad, T. J. Bunning, and R. A. Vaia, Appl. Phys. Lett. **85**, 6095 (2004).
[10]Y. J. Liu, X. W. Sun, P. Shum, H. P. Li, J. Mi, W. Ji, and X. H. Zhang, Appl. Phys. Lett. **88**, 061107 (2006).
[11]H. Kogelnik and C. V. Shank, J. Appl. Phys. **43**, 2327 (1972).
[12]M. Meier, A. Mekis, A. Dodabalapur, A. Timko, R. E. Slusher, J. D. Joannopoulos, and O. Nalamasu, Appl. Phys. Lett. **74**, 7 (1999).
[13]M. Notomi, H. Suzuki, and T. Tamamura, Appl. Phys. Lett. **78**, 1325 (2001).
[14]H.-Y. Ryu, S.-H. Kwon, Y.-J. Lee, Y.-H. Lee, and J.-S. Kim, Appl. Phys. Lett. **80**, 3476 (2002).
[15]S. Riechel, C. Kallinger, U. Lemmer, J. Feldmann, A. Gombert, V. Wittwer, and U. Scherf, Appl. Phys. Lett. **77**, 2310 (2000).
[16]V. Reboud, P. Lovera, N. Kehagias, M. Zelsmann, C. Schuster, F. Reuther, G. Gruetzner, G. Redmond, and C. M. Sotomayor Torres, Appl. Phys. Lett. **91**, 151101 (2007).
[17]M. B. Christiansen, A. Kristensen, S. Xiao, and N. A. Mortensen, Appl. Phys. Lett. **93**, 231101 (2008).
[18]K. Inoue, M. Sasada, J. Kawamata, K. Sakoda, and J. W. Haus, Jpn. J. Appl. Phys., Part 2 **38**, L157 (1999).
[19]R. Jakubiak, V. P. Tondiglia, L. V. Natarajan, R. L. Sutherland, P. Lloyd, T. J. Bunning, and R. A. Vaia, Adv. Mater. **17**, 2807 (2005).
[20]R. L. Sutherland, L. V. Natarajan, V. P. Tondiglia, and T. J. Bunning, Chem. Mater. **5**, 1533 (1993).
[21]M. Notomi, Phys. Rev. B **62**, 10696 (2000).
[22]K. Sakoda, K. Ohtaka, and T. Ueta, Opt. Express **4**, 481 (1999).